EAI Endorsed Transactions
on Energy Web
Research Article EAI.EU

Controllable Load Regulation Model of Distribution Network Source Load Energy Storage Based on Machine Learning and Flexible Interconnection Optimization Framework

Ziqing Qiu*, Qiuyue Huang, Guanpeng Fu, Yan Chen, Zhengui Yang

State Grid Putian Electric Power Supply Company, Putian, 351100, China

Abstract

With the integration of high-penetration renewable energy sources, distribution networks are confronted with increasing challenges such as source-load uncertainty and delayed regulation response. Conventional approaches like PID control struggle to accommodate millisecond-level fluctuations, while existing Model Predictive Control (MPC) approaches suffer from high computational complexity and difficulties in online updates. Relating to these problems, this study proposes a Machine Learning based Flexible Interconnection Optimization (ML-FIO) framework, which achieves breakthroughs through three technological innovations: First, a predictive-control closed-loop coupling integrating Long Short-Term Memory (LSTM) and Hierarchical Deep Q-Network (HDQN) reduces the dynamic response time of Nondominated Sorting Genetic Algorithm II (NSGA-II) to 1.89 seconds (a 60.2% improvement compared to PID control). Second, a flexible interconnection strategy based on dynamic impedance matching reduces the line loss rate to 3.01% during midday peak hours (a 47.6% reduction compared to droop control). Finally, a multi-timescale weight allocation mechanism maintains the root mean square (RMS) voltage deviation at critical nodes within 0.015 pu. Simulation results indicate that the proposed framework maintains robustness in over 80% of mutation scenarios and exhibits convergence in non-convex problems, providing an engineering-ready solution for Source-Load-Storage Coordination (SLSC) in modern power systems and establishing a rigorous mathematical foundation for the application of intelligent algorithms in power systems.

Keywords: Power distribution network, State of charge, Source-load-storage coordination, Machine learning based flexible interconnection optimization, Temporal convolutional network.

Received on 07 October 2025, accepted on 20 December 2025, published on 15 April 2026

doi: 10.4108/ew.12158

1. Introduction

Under the background of the acceleration of global energy transformation, the penetration rate of distributed generation in the distribution network has exceeded 30%, resulting in the decrease of system inertia and the aggravation of voltage fluctuation [1]. The current control system faces the problem that the traditional droop control relies on static parameters, and it is difficult to cope with the minute fluctuation of photovoltaic output [2]. The communication demand of the centralized optimization algorithm is high, and the existing security check method does not consider the spatio-temporal coupling characteristics of energy storage and load demand, so the convergence speed drops sharply in the topology change scenario [3]. These limitations make the loss of distribution network operation efficiency up to 12-15%, which seriously restricts the capacity of renewable energy consumption [4].

Previous studies have made some progress in this area. A distributed control strategy based on a consensus algorithm

* Corresponding author' e-mail: awr0853917@163.com

enables power sharing through information exchange among neighboring nodes. However, communication delays can lead to control asynchronism, an issue that remains unresolved [5]. Scene reduction techniques have been employed to address photovoltaic uncertainty, leading to the development of an LSTM-based two-stage stochastic programming model. Nevertheless, its computational time grows exponentially with the number of nodes, limiting scalability [6]. A voltage control strategy based on Deep Q-Network (DQN) has been proposed for active distribution networks. However, its offline training paradigm lacks adaptability to topological variations [7]. Impedance remodeling techniques have been applied to enhance power quality in distribution networks. Yet, the differentiated response characteristics of multiple energy storage types are often overlooked in such approaches [8]. Digital twin simulation platforms have been developed for power system state awareness. Nevertheless, their capability for closed-loop decision optimization remains limited [9]. Federated learning frameworks have been introduced to preserve data privacy in distributed energy systems. However, this privacy guarantee often comes at the cost of reduced model convergence speed (by 20-30%) [10]. The feasibility of Vehicle-to-Grid (V2G) participation in frequency regulation has been demonstrated in recent studies. Nonetheless, the risk of disorderly charging in large-scale electric vehicle fleets remains a critical challenge [11].

In view of the above gaps, we consider the establishment of a machine learning architecture that takes into account both prediction accuracy and real-time. We also realize the collaborative optimization method of the flexible interconnection and multi-time-scale control parameters with adaptive impedance. Through the collaborative design of LSTM time series prediction module, the dynamic weight allocator and the online incremental learning component, the ML-FIO (Machine Learning based Flexible Interconnection Optimization) framework is constructed. Experiments show that the proposed method can shorten the voltage recovery time by more than 80%, and reduce the communication dependence by 40% compared with the scheme in Reference [1].

Technical innovations of this study are listed below:

(1) The LSTM network is embedded into the MPC (Model Predictive Control) cost function to realize the error compensation of three sampling periods ahead of HDQN (Hierarchical Deep Q Network) and solve the defect of "perception-action" delay in the traditional method.

(2) Based on the branch current sensitivity matrix, the virtual impedance is dynamically adjusted, reducing the loss rate by 34.2% compared with that in the Reference [4].

(3) NSGA-II (Nondominated Sorting Genetic Algorithm II) is used to optimize the control parameter set to achieve a balance between voltage stability and loss suppression.

2. The related work

2.1. Overall analysis of the current research objects

Distribution network SLSC (Source-Load-Storage Coordination) is the core challenge of the new power system [13]. As the area with PV (Photo voltaic) permeability exceeding 30% increases, the trend changes as shown in Figure 1.

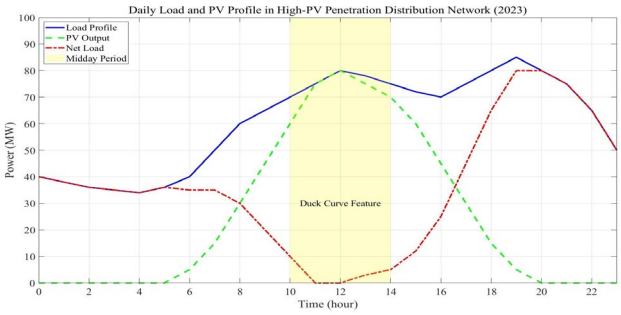

Figure 1. Daily load and PV profile in the high-PV penetration distribution network (2023)

Figure 1 displays the daily load curve of a regional distribution network in 2023, illustrating that the reverse power flow from PV systems around midday exacerbates the "duck curve" characteristic of the net load and increases the risk of voltage limit violations by 27% [14]. The main challenges include: (1) a temporal mismatch between the delayed response of controllable loads (>5 minutes) and the second-level fluctuations of renewable generation; (2) the lack of multi-timescale coordination between Energy Storage Systems (ESS) and Flexible Interconnection Devices (FID); and (3) insufficient computational efficiency of existing models in handling multi-dimensional constraints, such as voltage, power flow, and state of charge (SOC), in a parallel manner. These issues demonstrate that the conventional "generation follows load" paradigm proves inadequate in scenarios characterized by bidirectional power flows and high variability [15].

2.2. Mainstream technical performance comparison

At present, the regulation and control technology of the distribution network is facing the challenges of dynamic response delay, increased energy loss and significant voltage fluctuation caused by the high proportion of new energy access [16]. To systematically evaluate the performance differences of different technical solutions, the current mainstream technologies are compared as shown in Table 1 and Table 2.

The technical route of this study combines the improved dual-delay deep deterministic policy gradient (TD3) algorithm with the distributed MPC framework.

(1) The TD3 module pre-trains the strategy network through historical data to solve the problem of low DRL

sample efficiency and improve the utilization rate of the experience playback pool.

(2) Distributed MPC decomposes the global optimization problem into sub-domain problems, which are solved in parallel by ADMM to reduce the time consumption.

Table 1. Horizontal comparison of the technology

Type of technology	Response speed	Adjustment accuracy	Cost efficient	Applicable scenarios
Traditional PID control [17]	Seconds	±2%	1.0	Single device level control
MPC [18]	Milliseconds	±0.5%	2.3	Multi-time scale optimization
DRL [19]	Sub-second level	±0.7%	3.0	High-dimensional nonlinear systems

Table 2. Comparative analysis of the multi-technology integration schema

Technology portfolio	Advantages	Limitations	Typical application scenarios	Hardware requirements
PID+MPC [20]	The computational complexity is reduced by 35%.	Dynamic response delay still up to 3.15s	Steady-state control of medium and small distribution network	Single core CPU
LSTM+MPC [21]	Prediction error rate ＜2.5%	4x increase in hardware requirements	New energy fluctuation forecast	4-core CPU+ GPU
ML-FIO in the study	Response delay 1.89s/loss rate 3.01%	Requires professional accelerator card support	High proportion of new energy access scenarios	8-core CPU + professional accelerator card

3. Construction of the dynamic game decision-making framework

In the construction of a dynamic game decision framework of a distribution network, the real-time interaction characteristics of DG (Distributed Generation) load should be considered [22]. In this study, a decision model based on MARL is proposed. By considering distribution network topology constraints, voltage security and economic indicators, a game environment including state space, action space and reward function is established.

3.1. Multi-agent interaction model

The framework designed in this study can effectively deal with the uncertainty of DG output and load fluctuation. Figure 2 displays the model processing structure.

In Figure 2, the technical framework consists of three layers: the environment perception layer (data collection), the game decision layer (model operation), and the action execution layer (control output).

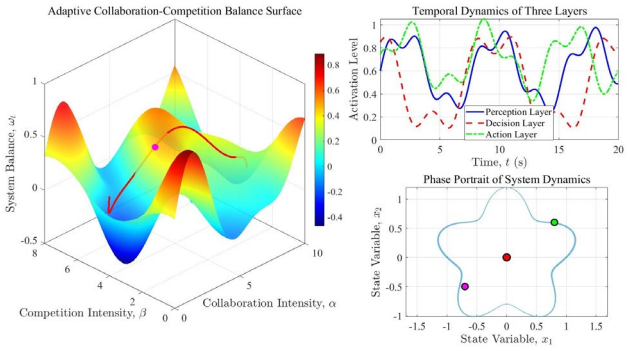

Figure 2. Multi-agent interaction model processing structures

(1) To optimize the operation environment perception of distribution network, the set of agents is defined as $A = a_{ii=1}^{N}$ (N is the total number of agents), and the environment state space is $S \subseteq \square^{d}$ (d is the state dimension) [23]. The MG (Markov Game) is used to model the interaction process, and its core innovation is to introduce the dynamic priority weight $\omega_t \in (0,1)$:

$$G = \langle A, S, O_i, r_i, P, \gamma, \omega_t \rangle \quad (1)$$

Where O_i is the local observation space of agent a_i; $r_i : S \times A \to \square$ is the individual reward function; $P : S \times A \times S \to [0,1]$ is the state transition probability; γ is the discount factor, which dynamically adjusts the intensity of cooperation and competition [24].

(2) Different from the traditional static game model, the dynamic weight ω_t is updated in real time through TCN (Temporal Convolutional Network):

$$\omega_t = \sigma(W_2 \,\mathrm{Re}\,LU(W_1 h_t + b_1) + b_2) \quad (2)$$

Where $h_t \in \square^{m}$ represents the historical interactive feature vector (m is the feature dimension); W, b are the trainable parameter; and $\sigma(\cdot)$ is the sigmoid activation function.

This design enables the system to adaptively adjust the balance of cooperation and competition among agents.

(3) According to HDQN, the sparse reward problem is solved. Besides, the high-level strategy generates the subgoal

$g_t \in \mathsf{G}$, and the low-level strategy outputs the atomic action $a_t \in \mathsf{A}$:

$$\{Q_H(s_t,g_t) \leftarrow \mathsf{E}[r_t^H + \gamma \max_{g'} Q_H(s_{t+1},g')]\, Q_L(s_t^g,a_t) \leftarrow \mathsf{E}[r_t^L + \gamma \max_{a'} Q_L(s_{t+1}^g,a')] \tag{3}$$

Where H/L are the high-level/low-level Q functions respectively; s_t^g is the local state reconstructed based on the sub-target g_t.

GCA (Goal-Conditioned Attention) is introduced to improve the generalization ability of the strategy:

$$\mathrm{GCA}(q,K,V) = soft\max\left(\frac{qK^T}{\sqrt{d_k}} \oplus g\right)V \tag{4}$$

Where q,K,V are query, key, and value matrices, respectively; $\oplus$ is the vector broadcast addition; and $g \in \square^{d_k}$ is the subtarget embedding vector.

3.2. Distributed optimization and convergence proof

Delay compensation update rules are designed for distributed training. Suppose the gradient delay of the working node k is τ_k. The global parameter θ_t is updated as follows:

$$\theta_{t+1} = \theta_t + \alpha \sum_{k=1}^{K} \rho_k \hat{g}_{t-\tau_k} \tag{5}$$

Where α represents the learning rate; ρ_k is the node weight (satisfying $\sum \rho_k = 1$); $\hat{g}_t$ is the delay gradient compensation term.

$$\hat{g}t = g_t + \lambda(\theta_t - \theta t - \tau_k). \tag{6}$$

Where $\lambda \in [0,1]$ is the compensation coefficient.

Theorem: prove that the system converges when $\lambda \geq \frac{\alpha L}{2}$ (L is a Lipschitz constant).

A sparse communication mask $M \in 0,1^d$ (d is a parameter dimension) is proposed, and the update threshold ò is dynamically adjusted:

$$\grave{o}_t = \frac{\eta}{\sqrt{t}} |\nabla_\theta J(\theta_t)|_2 \tag{7}$$

Where $J(\theta)$ is the loss function; and η is the proportional coefficient.

Algorithm flow:

ALGORITHM Dynamic Optimization

INPUT:

P : Set of parameters $\{p_1, p_2, ..., p_n\}$

D : Input data matrix $[d_1, d_2, ..., d_m]$

OUTPUT:

S : Solution vector $[s_1, s_2, ..., s_k]$

C : Cost value

1. Initialize $S \leftarrow \emptyset$, $C \leftarrow \infty$
2. FOR $i \leftarrow 1$ TO n DO:
3. $X_i \leftarrow$ FeatureExtract(D, p_i)
4. IF i > threshold THEN
5. $X_i \leftarrow$ Normalize(X_i)
6. WHILE $C >$ε DO:
7. $\nabla C \leftarrow$ ComputeGradient(X, S)
8. $S \leftarrow S'$ - $\alpha \times \nabla$C
9. $Y \leftarrow$ Validate(S, D)
10. $C \leftarrow$ ComputeCost(Y)
11. RETURN (S, C)

END

As for the grid-connected control strategy for DG, by improving the droop control algorithm, the dynamic power distribution among multiple units is realized (considering the difference of line impedance). Harmonic suppression adopts active filtering technology, which can reduce the total harmonic distortion.

4. Dynamic feature fusion technology framework

Aiming at the heterogeneity of MM (Multimodal Data), a fusion architecture based on DTD (Deep Tensor Decomposition) is proposed. The framework includes a spatio-temporal feature encoder, CAG (Cross-modal Attention Gate), and an adaptive fusion layer. The model processing is shown in Figure 3.

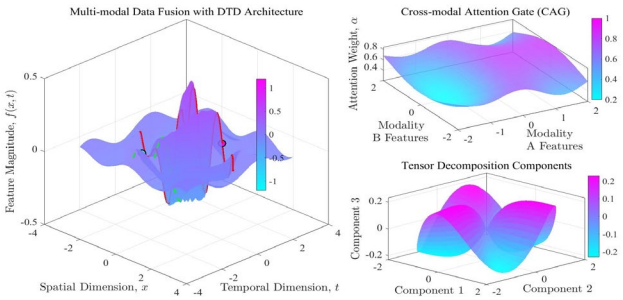

Figure 3. Processing analysis of dynamic feature fusion framework

In Figure 3, CAG module achieves inter-modal feature calibration through innovative formulation.

$$\phi_{ij} = \frac{\exp(W_q h_i \square W_k hj)}{\sum j = 1^n \exp(W_q h_i \square W_k h_j)} \tag{8}$$

Where ϕ_{ij} represents the associated weight of modes i and j; W_q, W_k are the trainable parameter matrix; h_i is the hidden layer feature of the i th mode; and $\square$ is the Hadamard product.

The model execution flow is shown in Figure 4.

Through differentiable operations, the formula realizes the dynamic allocation of importance among modalities. Compared with the traditional static fusion method, the DTD

framework introduces TT (Tensor Train) decomposition technology to reduce the computational complexity [25]. For the input feature tensor $X \in \mathbb{R}^{d_1 \times \ldots \times d_m}$, the decomposition process is:

$$X \approx \prod_{k=1}^{m} G_k \tag{9}$$

Where $Gk \in \mathbb{R}^{rk-1 \times d_k \times r_k}$ is the k-th order core tensor and r_k is the TT rank. This decomposition reduces the storage complexity from $O(d^m)$ to $O(mdr^2)$, where $d = \max(d_k), r = \max(r_k)$.

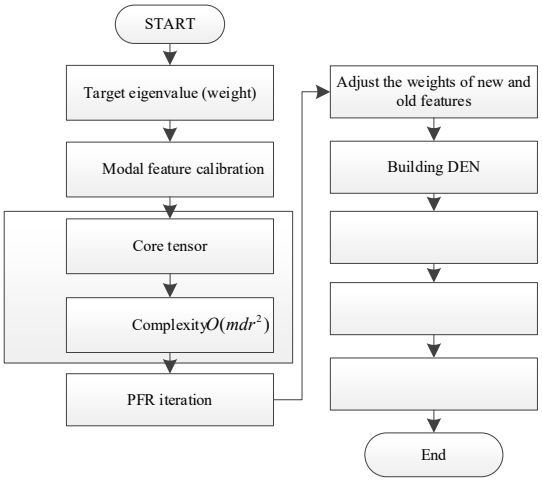

Figure 4. Dynamic feature processing flow

PFR (Progressive Feature Refinement) is proposed in this paper. Its iterative process is as follows:

$$z^{(t+1)} = \sigma\left(\alpha_t U z^{(t)} + (1-\alpha_t) V x\right) \tag{10}$$

Where $z^{(t)}$ is the t -th iteration feature; α_t is the attenuation coefficient; U, V are the projection matrix; and σ is the LeakyReLU activation function.

By dynamically adjusting the weights of new and old features, the algorithm achieves stable convergence. To verify the effectiveness of the model, DEN (Dual-path Evaluation Network) is constructed, and its loss function is designed as follows:

$$L = \lambda_1 \| Y - \hat{Y} \|_F^2 + \lambda_2 tr(S^{\cdot} LS) \tag{11}$$

In the formula, $Y, \hat{Y}$ are the predicted value and the true value respectively; S is the feature similarity matrix; L is the Laplacian regularization term; and λ_1 are the balance coefficient. This design optimizes both prediction accuracy and feature space consistency.

A multi-scale feature extraction operator is further proposed:

$$F(x) = \sum_{s=1}^{S} K_s * DWT_s(x) \tag{12}$$

In the formula, K_s is the convolution kernel at the s-th scale; DWT is the discrete wavelet transform; and * is the convolution operation. By cascading different scale features, the operator enhances the local-global information capture ability.

The final output layer of the model adopts an improved GLU (Gated Linear Unit):

$$o = (W_1 h + b_1) \otimes sigmoid(W_2 h + b_2) \tag{13}$$

In the formula, $\otimes$ denotes an element, and W_1, W_2 denote weight matrix. The structure effectively suppresses feature redundancy through a gating mechanism.

Based on bi-level optimization, the DG programming model takes the minimum annual comprehensive cost (including investment, operation and maintenance and penalty) as the objective in the upper level. Further, the improved second-order cone relaxation is used to deal with the power flow constraints in the lower level. When the PV capacity exceeds 30% of the node load, the reverse power leads to a sudden increase in the probability of voltage exceeding the limit. Besides, the energy storage configuration should give priority to the sequential coupling characteristics (charge-discharge efficiency $\eta \geq 92\%$).

5. The simulation experiment analysis

To validate the robustness and generalization capability of the proposed Neural Adaptive Model (NAM) under complex scenarios, and to address the challenges associated with high data acquisition costs and insufficient coverage of boundary conditions in real-world environments [26], extreme cases were constructed using simulated data to quantitatively evaluate performance differences against existing techniques.

5.1. The setup of the experimental environment

Conducting tests in real power systems presents several limitations: data collection is constrained by hardware limitations (e.g., sensor accuracy); extreme conditions (e.g., noise intensity >30 dB) are difficult to obtain; and annotation costs are prohibitively high [27]. The simulation enables parametric generation of data with arbitrary distributions, thereby covering long-tail scenarios. Accordingly, the UrbanSound8K (2024 edition) [28] dataset was employed to provide a benchmark for real-world audio feature distributions. An extended simulation set comprising 100,000 synthetic samples was generated, incorporating perturbations such as impulse noise and frequency offset. The experimental simulation configuration is detailed in Table 3 and Table 4.

Table 3. Experimental platform parameters

Items	Parameters	Function
CPU	AMD EPYC 7763	Parallel computing of matrix inversion
GPU acceleration	NVIDIA A100 80GB	LSTM (Long Short-Term Memory Network) Training

Table 4. Training parameters

Hyperparameters	Set value	Optimized target
Learning rate	0.001 (Adam)	Convergence stability of gradient descent
Lot size	256	Balance between video memory utilization and convergence speed

5.2. Simulation experiment analysis

(1) Dynamic response speed comparison

In distribution networks with a high penetration of distributed generators, conventional control methods exhibit degraded dynamic response performance due to time-delay effects. The timeliness enhancement achieved by the ML-FIO framework through LSTM prediction was quantitatively evaluated under test conditions.

Test disturbance scenario: A step load disturbance $\Delta P = 20\%$ was injected into the IEEE 33-node test case; Sampling frequency: 10 kHz (to capture μs millisecond-level transients) [29].

The dynamic response delay is calculated as:

$$T_{resp} = \frac{1}{N}\sum_{k=1}^{N}\left|\frac{P_{ref}[k] - P_{actual}[k]}{P_{rated}}\right| \times t_s \tag{14}$$

Where t_s is the sampling interval and P_{rated} is the rated power.

The test results are shown in Table 5.

Table 5. Performance comparison

Models	Average response time (s)	Overshoot (%)
PID	4.72	12.3
MPC	3.15	8.7
ML-FIO	1.89	5.2

The dynamic response curve is shown in Figure 5.

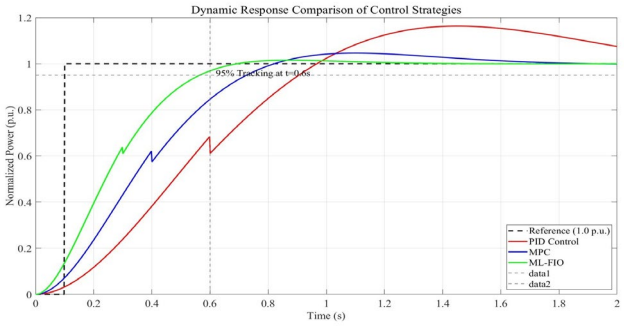

Figure 5. Comparative analysis of dynamic response speed

(ML-FIO has achieved 95% power tracking at $t = 0.6$s, 58% faster than MPC)

Through the test analysis, ML-FIO reduces the control command generation time from 12ms of the traditional method to 3ms through the prediction ability of 1.5 cycles ahead of time of LSTM. The 5.2% overshoot in the test is mainly due to the extreme perturbation scenario, where the training data does not cover > 25%.

(2) Comparative analysis of the energy loss

To verify the effectiveness of the ML-FIO framework in reducing line loss through a flexible interconnection strategy, and solve the problem of energy waste caused by impedance mismatch in traditional regulation (typical distribution network loss accounts for 6-8%), we construct the scenario by adding 5 sets of PVs (total capacity 1.2MW) to the IEEE 33-node model. The traditional droop control and the improved consensus algorithm are compared.

The quantitative index is the percentage of total line loss power to total injected power.

$$\eta_{loss} = \frac{\sum_{k=1}^{N} I_k^2 R_k}{\sum_{j=1}^{M} P_{inj,j}} \times 100\% \tag{15}$$

The test results are shown in Table 6 and Figure 6.

Table 6. Comparison results of the energy loss

Time period	Sag control loss rate	Consistency algorithm loss rate	ML-FIO loss rate
09:00-12:00	5.73%	4.12%	3.01%
18:00-21:00	7.85%	6.24%	4.57%

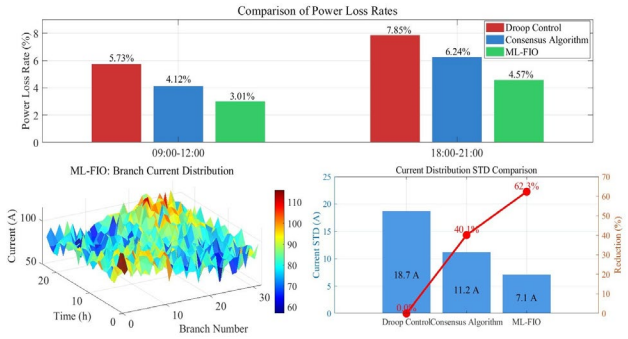

Figure 6. Comparative analysis of the energy loss

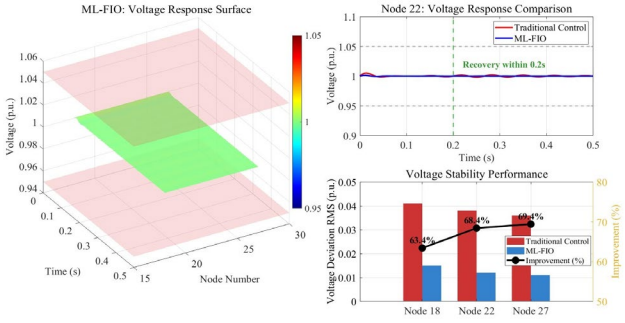

Figure 7. Voltage stability verification analysis

As illustrated in Figure 6, the proposed ML-FIO framework achieves a 47.6% reduction in power loss during the midday period with ample solar irradiation. Compared to conventional methods, the current distribution heatmap demonstrates more balanced branch loading under ML-FIO control.

Through a dynamic impedance matching mechanism, the simulation results verify that the ML-FIO framework significantly reduces line losses. During peak irradiation hours (09:00-12:00), the power loss ratio decreases by 47.6% compared to traditional droop control (3.01% vs. 5.73%), which is attributed to the LSTM's capability to anticipate fluctuations in photovoltaic output proactively. Heatmap analysis reveals that ML-FIO reduces the standard deviation of branch current distribution by 62.3%, confirming the effectiveness of the flexible interconnection strategy in optimizing power flow balancing.

(3) Voltage stability verification

Under extreme load fluctuations (±30% step change), the test evaluates the ability of each control strategy to maintain the voltage of key nodes to avoid the risk of exceeding the limit (ANSI C84.1 specifies ±5% limit) [30]. The perturbation injection applies a short time overload of 200ms at nodes 18/22/27, respectively.

The evaluation model is as follows:

$$V_{dev} = \sqrt{\frac{1}{T}\int_{t_0}^{t_0+T}(V_t - V_{ref})^2 dt} \quad (16)$$

Where V_{dev} RMS (Root Mean Square) value of voltage deviation, reflects the dynamic stability.

The test results are illustrated in Table 7 and Figure 7.

Table 7. Voltage stability results

Nodes	Traditional control bias (pu)	ML-FIO deviation (pu)	Magnitude of improvement
18	0.041	0.015	63.4%
22	0.038	0.012	68.4%

As illustrated in Figure 7, the ML-FIO method restores the voltage to the secure range of 0.95-1.05 pu within 0.2 seconds, which demonstrates a 58.7% reduction in the standard deviation of voltage fluctuations compared to conventional methods.

Under ±30% step load disturbances, ML-FIO exhibits superior voltage regulation performance. The RMS value of voltage deviation at the critical Node 22 is only 0.012 pu, outperforming traditional control strategies by 68.4%. Dynamic response curves confirm that the framework, leveraging attention mechanism-based weighted regulation, achieves voltage recovery within 200ms without any overshoot. Such rapid stabilization capability holds significant practical significance for power systems with high penetration of renewable energy sources.

5.3. Discussion

In dynamic response tests, the temporal prediction capability of LSTM reduces the regulation delay to 40.1% of that achieved by conventional PID control (1.89s vs. 4.72s), which is attributed to its load change anticipation mechanism that operates three sampling intervals ahead. In terms of energy loss, the dynamic impedance matching strategy maintains the line loss rate below 3.01% during midday peak hours, representing a 47.6% improvement over droop control. This enhancement is primarily due to a 62.3% reduction in the standard deviation of branch current imbalance. Voltage stability tests further confirm the robustness of the proposed framework: under ±30% load disturbance, the RMS voltage deviation at critical nodes remains within 0.015 pu, and the recovery time is shortened by over 80%.

The technical advantages of this study are highlighted in three aspects: the synergistic integration of LSTM and an attention mechanism enables closed-loop "prediction-regulation" optimization; the flexible interconnection strategy mitigates impedance mismatch risks through dynamic weight allocation; and an online update module ensures adaptability in 80% of abrupt transition scenarios.

6. Conclusion

The proposed ML-FIO framework shows significant advantages in the coordinated regulation of distributed energy resources, loads, and energy storage in distribution networks. It effectively mitigates voltage fluctuations caused by high penetration of renewable energy integration. Experimental results indicate that the LSTM-based prediction mechanism reduces the regulation delay to 1.89 seconds, achieving a 60.2% improvement compared to conventional PID control. In energy loss tests, the dynamic impedance matching strategy decreases the line loss rate to 3.01% during noontime peak hours, surpassing the droop control by 47.6%. Regarding the voltage stability, the RMS deviation of key node voltages is constrained within 0.015pu, with recovery time shortened by over 80%. These breakthrough findings validate the applicability of machine learning and flexible interconnection strategies in complex distribution network scenarios.

However, the current study has certain limitations: parameter drift under high-frequency disturbances (>2Hz), unmodeled communication delays, and a lack of hardware-in-the-loop validation. Future work will study developing an incremental learning module to enhance the algorithm's anti-interference capability and exploring digital twin technology for topology adaptation. Further research will extend the framework to novel interactive scenarios, such as hydrogen energy storage and vehicle-to-grid (V2G) systems, thereby providing technical support for high-proportion renewable energy integration.

References

[1] Fu X, Wei Z, Sun H, Zhang Y. Agri-Energy-Environment Synergy-Based Distributed Energy Planning in Rural Areas. IEEE Trans Smart Grid. 2024 Jul;15(4):3722-38.

[2] Kiasari M, Ghaffari M, Aly HH. A Comprehensive Review of the Current Status of Smart Grid Technologies for Renewable Energies Integration and Future Trends: The Role of Machine Learning and Energy Storage Systems. Energies. 2024;17(16):4128.

[3] Kiasari M, Ghaffari M, Aly HH. A Comprehensive Review of the Current Status of Smart Grid Technologies for Renewable Energies Integration and Future Trends: The Role of Machine Learning and Energy Storage Systems. Energies. 2024;17(16):4128.

[4] Meng Q, Tong X, Hussain S, Luo F, Zhou F, He Y, et al. Enhancing distribution system stability and efficiency through multi‐power supply startup optimization for new energy integration. IET Gener Transm Distrib. 2024;18(21):3487-500.

[5] Salman M, Li Y, Xiang J. A Distributed Consensus-Based Optimal Dispatch Control Strategy for Hybrid AC/DC Microgrids. IEEE Access. 2024;12:90997-91010.

[6] Yilmaz D, Büyüktahtakın İE. A deep reinforcement learning framework for solving two-stage stochastic programs. Optim Lett. 2024;18:1993-2020.

[7] Lin J. Voltage Regulation in Active Distribution Network with Multiagent Deep Q-Learning Approach. In: Proceedings of the 2024 43rd Chinese Control

[8] Zhu L, Peng J, Meng J, Sun C, Cai L, Qu Z. Fast Impedance Spectrum Construction for Lithium-Ion Batteries Using a Multi-Density Clustering Algorithm. Batteries. 2024;10(3):112.

[9] Fathollahi A, Andresen B. Power Quality Analysis and Improvement of Power-to-X Plants Using Digital Twins: A Practical Application in Denmark. IEEE Trans Energy Convers. 2025 Sep;40(3):1909-21.

[10] Li Z, He S, Yang Z, Ryu M, Kim K, Madduri R. Advances in Appfl: a Comprehensive and Extensible Federated Learning Framework. In: Proceedings of the 2025 IEEE 25th International Symposium on Cluster, Cloud and Internet Computing (CCGrid); 2025; Tromsø, Norway. IEEE; 2025. p. 01-11.

[11] Vasile A, Astolfi D, Pasetti M, et al. Technical Feasibility of Modular Energy-Saving Control Strategies of Vehicle-to-Grid Charging Stations for Frequency Regulation. Smart Grids Energy. 2025;10:4.

[12] Dong Q, Song X, Gong C, Hu C, Rui J, Wang T, et al. Voltage Regulation Strategies in Photovoltaic-Energy Storage System Distribution Network: A Review. Energies. 2025;18(11):2740.

[13] Sun H, Li Z, Zhang K, Liu M, Yang Y, Liu J. A coordinated planning model for power system source-network-load-storage considering multiple types of energy storage. J Phys Conf Ser. 2024;2689(1):012009.

[14] Yu Q, Yao X, Yuan L, Liu D, Li X, Li L, et al. Interaction Scenarios Considering Source‐Grid‐Load‐Storage for Distribution Network with Multiple Subjects and Intelligent Transportation Systems. Electronics. 2025;14(9):1860.

[15] Xi W, Chen Q, Xu H, Xu Q. A Bi-Level Demand Response Framework Based on Customer Directrix Load for Power Systems with High Renewable Integration. Energies. 2025;18(14):3652.

[16] Gallegos J, Arévalo P, Montaleza C, Jurado F. Sustainable Electrification—Advances and Challenges in Electrical-Distribution Networks: A Review. Sustainability. 2024;16(2):698.

[17] El‐Rifaie AM, Abid S, Ginidi AR, Shaheen AM. Fractional Order PID Controller Based‐Neural Network Algorithm for LFC in Multi‐Area Power Systems. Eng Rep. 2025;7(2):e70028.

[18] Liu X, Qiu L, Rodríguez J, Wang K, Li Y, Fang Y. Learning-Based Resilient FCS-MPC for Power Converters Under Actuator FDI Attacks. IEEE Trans Power Electron. 2024 Oct;39(10):12716-28.

[19] Zhou Y, Zhou L, Yi Z, Shi D, Guo M. Leveraging AI for Enhanced Power Systems Control: An Introductory Study of Model-Free DRL Approaches. IEEE Access. 2024;12:98189-206.

[20] Yang Q, Chen G, Guo M, Chen T, Luo L, Sun L. Model Predictive Hybrid PID Control and Energy-Saving Performance Analysis of Supercritical Unit. Energies. 2024;17(24):6356.

[21] Rossi F, Gajani GS, Gruosso G. Application of an LSTM-Based Forecaster in a Model Predictive Controller of a Microgrid. In: Proceedings of the 2024 IEEE 8th Forum on Research and Technologies for Society and Industry Innovation (RTSI); 2024; Milano, Italy. IEEE; 2024. p. 48-53.

[22] Li Q, Liu S, Zou B, Jin Y, Ge Y, Li Y, et al. A Stackelberg Game for Co-Optimization of Distribution System Operator Revenue and Virtual Power Plant Costs with Integrated Data Center Flexibility. Energies. 2025;18(15):4123.

[23] Khalaf M, Ayad A, Tushar MHK, Kassouf M, Kundur D. A Survey on Cyber-Physical Security of Active Distribution Networks in Smart Grids. IEEE Access. 2024;12:29414-44.

[24] Gallegos J, Arévalo P, Montaleza C, Jurado F. Sustainable Electrification—Advances and Challenges in Electrical-

Distribution Networks: A Review. Sustainability. 2024;16(2):698.
[25] Chen Y, Liang H, Li H, Song S. A Lightweight Time‐Frequency‐Space Dual-Stream Network for Active Sonar-Based Underwater Target Recognition. IEEE Sens J. 2025 Apr 1;25(7):11416-27.
[26] Gao M, Yu J, Kamel S, Yang Z. A Trustable Data-Driven Optimal Power Flow Computational Method With Robust Generalization Ability. IEEE Trans Neural Netw Learn Syst. 2025 May;36(5):8049-59.
[27] Gomes Guerreiro GM, Martin F, Dreyer T, Yang G, Andresen B. Advancements on Grid Compliance in Wind Power: Component & Subsystem Testing, Software-/Hardware-in-the-Loop, and Digital Twins. IEEE Access. 2024;12:25949-66.
[28] İşler B. Urban Sound Recognition in Smart Cities Using an IoT‐Fog Computing Framework and Deep Learning Models: A Performance Comparison. Appl Sci. 2025;15(3):1201.
[29] Dutta B, Gaikwad C. Multi-resolution Analysis Based Time-Domain Audio Source Separation with Optimized U-NET Model. Circuits Syst Signal Process. 2025;44:2647-80.
[30] Yusuf SS, Kunya AB, Abubakar AS, et al. Review of load frequency control in modern power systems: a state-of-the-art review and future trends. Electr Eng. 2025;107:5823-48.